GEOPHYSICS, VOL. 76, NO. 4 (JULY-AUGUST 2011); P. G73–G83, 8 FIGS., 2 TABLES.
10.1190/1.3581094

A laboratory study of NMR relaxation times in unconsolidated heterogeneous sediments

Elliot Grunewald[1] and Rosemary Knight[1]

ABSTRACT

Nuclear magnetic resonance (NMR) relaxation-time measurements can provide critical information about the physiochemical properties of water-saturated media and are used often to characterize geologic materials. In unconsolidated sediments, the link between measured relaxation times and pore-scale properties can be complicated when diffusing water molecules couple the relaxation response of heterogeneous regions within a well-connected pore space. Controlled laboratory experiments have allowed us to investigate what factors control the extent of diffusional coupling in unconsolidated sediments and what information is conveyed by the relaxation-time distribution under varied conditions. A range of sediment samples exhibiting heterogeneity in the form of a bimodal mineralogy of quartz and hematite were mixed with varied mineral concentration and grain size. NMR relaxation measurements and geometric analysis of these mixtures demonstrate the importance of two critical length scales controlling the relaxation response: the diffusion length ℓ_D, describing the distance a water molecule diffuses during the NMR measurement, and the separation length ℓ_S, describing the scale at which heterogeneity occurs. For the condition of $\ell_S > \ell_D$, which prevails for samples with low hematite concentrations and coarser grain size, coupling is weak and the bimodal relaxation-time distribution independently reflects the relaxation properties of the two mineral constituents in the heterogeneous mixtures. For the condition of $\ell_S < \ell_D$, which prevails at higher hematite concentrations and finer grain size, the relaxation-time distribution no longer reflects the presence of a bimodal mineralogy but instead conveys a more complex averaging of the heterogeneous relaxation environments. This study has shown the potential extent and influence of diffusional coupling in unconsolidated heterogeneous sediments, and can serve to inform the interpretation of NMR measurements in near-surface environments where unconsolidated sediments are commonly encountered.

INTRODUCTION

Nuclear magnetic resonance (NMR) relaxation measurements are highly sensitive to the pore-scale properties of geologic media. These methods probe the time required for hydrogen nuclei or "spins" in fluids to relax to equilibrium through diffusion and interaction with the physiochemical pore environment. Applications of NMR in petroleum well logging over the past several decades have demonstrated robust links between measured relaxation times and important formation properties, including pore size and permeability (Seevers, 1966; Timur, 1969; Kenyon et al., 1988). Recently, NMR logging has been extended to near-surface applications (Maliva et al., 2009; Walsh et al., 2010), and surface-based NMR instruments have been developed to characterize groundwater aquifers noninvasively (Legchenko and Valla, 2002; Hertrich, 2008; Walsh 2008). The types of materials encountered in near-surface environments, however, can differ significantly from those considered in oil and gas reservoirs. The goal of this study is to inform the interpretation of NMR measurements in the near surface by directly exploring the relaxation response of a specific class of media ubiquitous in these environments: unconsolidated heterogeneous sediments.

One fundamental difference between near-surface sediments and the lithologies typically encountered in oil and gas applications is the degree to which the pore space is connected. The conventional interpretation of NMR relaxation data assumes that each diffusing spin samples only one pore environment during the measurement; thus, the relaxation-time distribution is taken as a direct representation of the distribution of pore types. Although this assumption is generally valid for consolidated

Manuscript received by the Editor 28 June 2010; revised manuscript received 20 November 2010; published online 3 June 2011.
[1]Stanford University, Department of Geophysics, Stanford, California, U.S.A. E-mail: elliotg@stanford.edu; rknight@stanford.edu.
© 2011 Society of Exploration Geophysicists. All rights reserved.

Downloaded 06 Oct 2011 to 171.67.216.22. Redistribution subject to SEG license or copyright; see Terms of Use at http://segdl.org/

rocks, if the pore network is very well connected, diffusing spins can sample multiple physiochemical environments before relaxing. In this case, heterogeneous regions of the pore space will be coupled by diffusion and the relaxation-time distribution will represent a more complex averaging of the underlying heterogeneity, masking the true distribution of pore-scale properties. Because unconsolidated sediments typically possess a very open pore network, it is likely that diffusional coupling effects will be particularly prevalent in these materials.

Assessing the influence of diffusional coupling on the NMR relaxation response in unconsolidated sediments is critical to advancing the application of this method in near-surface environments. Several studies have explored diffusional coupling from a theoretical approach by considering relaxation in idealized pore networks (Cohen and Mendelson, 1982; McCall et al., 1991; Zielinski et al., 2002). Previous laboratory studies, on the other hand, have primarily aimed to characterize coupling effects in synthetic media (D'Orazio et al., 1989) or lithologies of particular significance in hydrocarbon reservoirs, namely carbonates (Toumelin et al., 2002) and shaley sandstones (Anand and Hirasaki, 2007; Fleury and Soualem, 2009). Although these studies do not directly consider the NMR relaxation response in unconsolidated sediments, they highlight the importance of generalized time and length scales that control the degree to which diffusional coupling will influence measured relaxation times.

Based on these studies, we can distinguish two fundamental length scales that are critical to the coupling process: the diffusion length ℓ_D and the separation length ℓ_S; we illustrate these length scales in Figure 1. We show a porous medium composed of heterogeneous regions, represented by two shades of gray, where the heterogeneity can be in any physical, chemical, or geologic property that influences NMR relaxation. The first length scale ℓ_D, represented by the dimension of the dashed circles, describes the distance a spin can sample by diffusion before relaxing. The second length scale ℓ_S is associated with the scale of heterogeneity and describes the distance a diffusing spin must travel to sample more than one relaxation environment. If $\ell_S < \ell_D$, as is the case in Figure 1a, the majority of spins sample more than one relaxation environment and diffusional coupling will strongly influence the NMR relaxation response. The extent of coupling can vary as a function of either of these key length scales. If ℓ_D increases (as shown in Figure 1b) or if ℓ_S decreases (as shown in Figure 1c) so that spins primarily sample only one relaxation environment, the extent of coupling will be more limited.

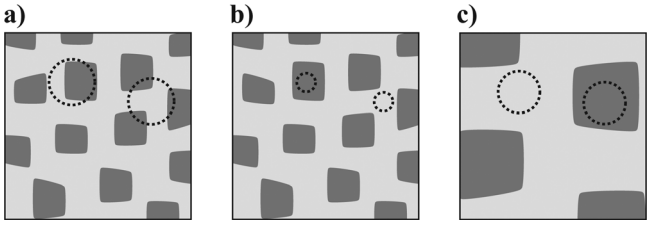

Figure 1. Schematic illustration of the length scales controlling diffusional coupling in a heterogeneous medium for three cases. Heterogeneous regions of the pore space are represented by different shades of gray. The length scale ℓ_D is represented by the dimension of the dashed circle; the length scale ℓ_S is described by the scale of the heterogeneous features. In (a), the condition $\ell_S > \ell_D$ is satisfied and diffusional coupling is significant. The extent of coupling is reduced when (b) ℓ_D decreases or (c) ℓ_S increases.

Using controlled laboratory experiments and analytic modeling, we aim to determine how these key length scales influence the extent of diffusional coupling and the information that is captured by the NMR relaxation response. In a previous laboratory study, we investigate systems represented by Figure 1a and 1b, in which the extent of coupling varies as a function of ℓ_D (Grunewald and Knight, 2009). Using synthetic silica gels with a bimodal pore-size distribution, we conclusively demonstrate that surface geochemistry can control ℓ_D and thus the impact of diffusional coupling. By sorbing varied amounts of iron(III) to the solid surface, we synthesize samples exhibiting a range of coupling strengths and illustrate how ℓ_D and coupling affects the NMR relaxation response in these well-characterized materials. We recognize that in natural sediments, the scale at which heterogeneity occurs, represented by ℓ_S, might vary much more than ℓ_D, and thus this length scale is likely to control the influence of diffusional coupling in many near-surface materials.

In the present laboratory study, we systematically explore the relaxation response of heterogeneous unconsolidated sediments between which the scale of heterogeneity varies. We consider realistic unconsolidated samples in which heterogeneity is present in the form of a bimodal grain mineralogy. We show that by varying the relative mineral concentrations and grain size, we create a range of samples between which the extent of coupling varies with the relative magnitude of ℓ_D and ℓ_S. Comparing these samples allows us to demonstrate how heterogeneity is reflected by the relaxation-time distribution over a range of conditions. These experiments provide direct insights into the relaxation response of unconsolidated heterogeneous sediments and thus inform the interpretation of NMR measurements in near-surface environments.

BACKGROUND

NMR relaxation theory

The NMR relaxation measurement probes the response of hydrogen nuclei in pore fluids to a magnetic field perturbation. At equilibrium with a static magnetic field, spin magnetic moments associated with hydrogen nuclei align, giving rise to a net nuclear magnetization parallel to the static field. In the standard NMR measurement, these spins are perturbed from the equilibrium state by the application of a short oscillating electromagnetic pulse. The pulse excites the spins to a higher energy state, and a detectable change in the nuclear magnetization signal is monitored over time t as the system relaxes back to equilibrium.

The NMR relaxation behavior is characterized by two different parameters: the longitudinal relaxation time T_1 and the transverse relaxation time T_2. In this study, we exclusively consider T_2, which is of great relevance to well-logging and surface-based NMR applications. For a single fluid-saturated pore, the net observed relaxation rate T_2^{-1} represents the sum of three relaxation mechanisms acting in parallel, each with a characteristic rate (Kleinberg and Horsfield, 1990):

$$T_2^{-1} = T_{2B}^{-1} + T_{2S}^{-1} + T_{2D}^{-1} \quad (1)$$

Here T_{2B}^{-1} is the bulk fluid relaxation rate, T_{2S}^{-1} is the surface relaxation rate, and T_{2D}^{-1} is the diffusion relaxation rate.

Downloaded 06 Oct 2011 to 171.67.216.22. Redistribution subject to SEG license or copyright; see Terms of Use at http://segdl.org/

Bulk fluid relaxation occurs due to molecular interactions within the fluid and is independent of the pore space. The magnitude of T_{2B}^{-1} depends primarily on the fluid viscosity and the concentration of dissolved paramagnetic species, such as Mn^{2+} and Fe^{3+} (Bloembergen et al., 1948). Diffusion relaxation occurs as spins diffuse in the presence of a spatially variable magnetic field. The magnitude of T_{2D}^{-1} is given by

$$T_{2D}^{-1} = \frac{D}{12}(\gamma G t_E)^2 , \tag{2}$$

where D is the diffusion coefficient of the fluid; G is the average magnetic field gradient; γ is the gyromagnetic ratio; and t_E is the echo time, a parameter of the Carr-Purcell-Meiboom-Gill (CPMG) measurement sequence (Carr and Purcell, 1954; Meiboom and Gill, 1958). In water-saturated geologic materials that are weakly magnetic, T_{2B}^{-1} and T_{2D}^{-1} are negligible, and the expression for T_2^{-1} is dominated by surface relaxation.

Surface relaxation occurs due to interactions between diffusing spins and the grain surfaces. In the condition of "fast diffusion" (Senturia and Robinson, 1970; Brownstein and Tarr, 1979), the magnitude of T_{2S}^{-1} is given by

$$T_{2S}^{-1} = T_{2S,fast}^{-1} = \rho S/V , \tag{3}$$

where S/V is the surface-area-to-volume ratio of the pore and ρ is the surface relaxivity. In general, S/V is inversely proportional to the pore size; for a spherical pore of radius r, the value of S/V is given by $3/r$. The magnitude of ρ describes the capacity of the grain surface to enhance relaxation and generally increases with the concentration of paramagnetic sites on the grain surface (Foley et al., 1996; Bryar et al., 2000).

The fast-diffusion regime, in which equation 3 is valid, requires that spins can diffuse to relaxation sites on the grain surface much more rapidly than they undergo relaxation at the surface; as described by Brownstein and Tarr (1979), this condition is satisfied for $\rho r/D \ll 1$. If alternately, spins undergo relaxation at the surface much more rapidly than they can diffuse to the surface ($\rho r/D \gg 10$), relaxation occurs in the slow-diffusion regime. In the slow-diffusion regime, surface relaxation does not occur at a single rate, but instead exhibits multiple relaxation modes with different decay rates. The dominant rate at which most relaxation occurs is inversely proportional to the mean-squared distance a spin must diffuse to reach the relaxation surface. For a spherical pore, the dominant slow-diffusion relaxation rate is given by

$$T_{2S}^{-1} = T_{2S,slow}^{-1} = \frac{6D}{r^2} \tag{4}$$

(Godefroy et al., 2001). Whereas most of the magnetization signal relaxes at this rate $T_{2S,slow}^{-1}$, a portion of the signal also relaxes in higher order modes exhibiting faster rates, the magnitudes of which depend on ρ. At intermediate values of $1 < \rho r/D < 10$, the rate of the dominant relaxation mode is between $T_{2S,fast}^{-1}$ and $T_{2S,slow}^{-1}$, and a smaller portion of the signal relaxes in higher order modes.

NMR relaxation in heterogeneous media

For a single water-filled pore in the fast-diffusion limit, the measured transverse magnetization signal $M(t)$ exhibits an exponential decay:

$$M(t) = Ae^{-t/T_2} , \tag{5}$$

where the initial amplitude A is proportional to the number of hydrogen spins (i.e., the pore volume). For a rock or sediment with multiple pore types, the observed signal generally exhibits a multiexponential decay:

$$M(t) = \sum_i A_i e^{-t/T_{2i}} . \tag{6}$$

Here, the amplitude A_i is proportional to the portion of signal relaxing at a mode with the corresponding decay time T_{2i}. A T_2 distribution is obtained from the measured $M(t)$ data by applying a Laplace inversion.

Conventionally, pore-scale properties are estimated from the T_2 distribution under two fundamental assumptions. The first assumption is that T_2 is controlled by surface relaxation in the fast-diffusion limit (equation 3). The second critical assumption is that each spin samples only one pore environment, and thus each pore contributes in isolation to the measured signal. Considering pores as such, to be theoretically isolated, each peak in the distribution of T_2 values is interpreted to represent a unique pore environment with different S/V or ρ; in some cases (e.g., deriving permeability), the mean log relaxation time T_{2ml} is calculated from the distribution to determine an average value of S/V or ρ. Thus, information about the distribution of pore sizes (e.g., Gallegos and Smith, 1988) or surface geochemistry (e.g., Keating et al., 2008) is extracted directly from the distribution of relaxation times.

In many rocks, these basic assumptions are approximately valid: weak relaxation surfaces are uniformly distributed (i.e., satisfying the conditions for fast diffusion), and constrictive pore throats limit spins from diffusing between pores. For reservoir sandstones in particular, numerous studies have shown that the T_2 distribution directly reflects the underlying pore-size distribution (e.g., Davies, 1990; Borgia et al., 1996). The assumptions are not always appropriate, however, for materials in which spins can readily diffuse between heterogeneous pore environments. As an example, for carbonate grainstones (Toumelin et al., 2002) and synthetic silica gels (Anand and Hirasaki, 2007; Grunewald and Knight, 2009), in which closely connected micropores and macropores are strongly coupled by diffusion, peaks in the T_2 distribution do not accurately capture the properties of either pore type. For unconsolidated near-surface sediments of interest in this study, we anticipate that spins will be able to diffuse readily between heterogeneous environments with different geometry (S/V) or mineralogy (ρ).

Referring back to Figure 1, let us consider in more detail the two length scales controlling the extent of diffusional coupling. The magnitude of the diffusion length ℓ_D describes the average distance a spin can diffuse during a time interval T of the NMR measurement, and can be estimated from the Einstein equation for self-diffusion,

$$\ell_D = \sqrt{6DT} . \tag{7}$$

Considering the time required for a spin to relax as characterized by T_2 (typically 1 to 1000 ms) and a typical value of D (2.46×10^{-9} m^2/s, the self-diffusion coefficient of water at 30°C; Simpson and Carr, 1958), the dimension of the region sampled by a diffusing spin during the NMR measurement can be greater than 100 μm. The second critical scale ℓ_S is a

Downloaded 06 Oct 2011 to 171.67.216.22. Redistribution subject to SEG license or copyright; see Terms of Use at http://segdl.org/

measure of the separation distance between heterogeneous regions of the pore space, where the heterogeneity results in different relaxation properties (i.e., different S/V or ρ). D'Orazio et al. (1989) explain that if dissimilar relaxation environments are separated by a distance shorter than the diffusion length (i.e., $\ell_S < \ell_D$), spins will sample multiple relaxation environments and the relaxation-time distribution will represent an averaging of these environments as a result of diffusional coupling.

In our experiments, we explore the importance of these length scales and the influence of diffusional coupling on NMR relaxation times in unconsolidated sediments with a heterogeneous mineralogy. Using mixtures of quartz and hematite, we prepared samples between which we directly vary ℓ_S by varying the volume concentrations of the minerals and the mean grain size. Figure 2a schematically illustrates the significance of ℓ_S and ℓ_D in these mixtures; the two minerals are represented by gray and black grains. For the system shown at the top, the average distance separating the gray and black grains is much greater than the diffusion length (represented by the dimension of the dashed circles); therefore, most spins will sample only one mineralogy before relaxing and diffusional coupling is expected to be weak. We expect that if the concentration of black grains increases (bottom left panel) or the mean grain size decreases (bottom right panel), ℓ_S will shorten. As illustrated in Figure 2b, we anticipate a critical threshold will exist when ℓ_S becomes shorter than ℓ_D, at which point diffusional coupling effects will begin to influence the relaxation response as spins become able to sample both mineralogies before relaxing. Thus, analyzing the NMR relaxation response for this suite of samples with varied mineral concentration and grain size allows us to explore systematically how heterogeneity is represented by the relaxation-time distribution in unconsolidated sediments over a wide range of conditions.

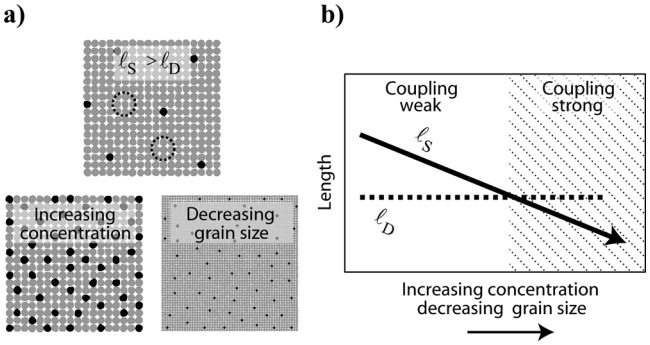

Figure 2. Schematic illustration of the factors expected to control diffusional coupling in sediments with a bimodal mineralogy. (a) Three cases are shown with gray and black grains representing two different mineralogies. In the top panel, ℓ_S is greater than the diffusion length ℓ_D. Increasing the concentration of black grains (bottom left panel), or decreasing the mean grain size (bottom right panel), decreases ℓ_S. (b) The length scale ℓ_S (solid line) decreases relative to ℓ_D (dashed line) as a function of grain size and mineral concentration. Hatch marks indicate the condition $\ell_S < \ell_D$, for which diffusional coupling is predicted to occur.

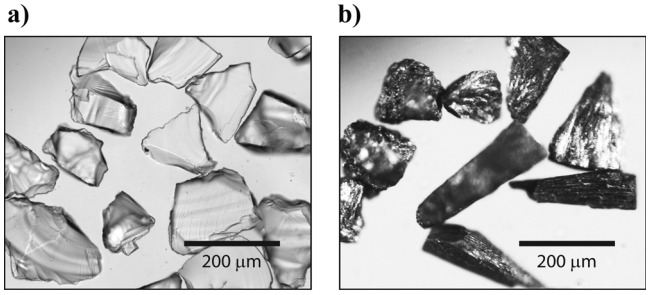

Figure 3. Optical microscope images of the (a) coarse quartz grains and (b) coarse hematite grains.

MATERIALS AND METHODS

Sample preparation and characterization

For our laboratory experiments, we prepared grain packs having a bimodal mineralogy of quartz (SiO_2) and hematite (Fe_2O_3). Quartz and hematite were selected because these minerals exhibit very different ρ values; Keating and Knight (2007) find that the ρ value for quartz grains increases by nearly two orders of magnitude when hematite surface coatings are applied. Both of these minerals are also commonly encountered in near-surface sediments; quartz is one of the most abundant minerals in earth's crust; hematite is found in soils and sediments at concentrations as high as 10% and often is formed by the oxidation of many other iron-bearing minerals (Stucki et al., 1988). An additional reason for selecting hematite is its low magnetic susceptibility relative to other iron minerals; hematite thus is not expected to introduce significant magnetic effects (entering through the T_{2D}^{-1} term) that would complicate our interpretation.

The quartz grains used here were derived from high-purity fused silicon dioxide pellets received from Sigma-Aldrich (4–16 mesh size, 99.9% SiO_2). Hematite grains were derived from a natural botryoidal hematite specimen received from Gem & Mineral Miners, Inc. (mined from an ore deposit in Alnif, Errachidia Province, Morocco). The original mineral materials were crushed first by rock hammer and then by mortar and pestle to obtain sand-sized grains. An alumina ceramic rock grinder was used to reduce the grain size further. We sorted the crushed minerals by grain diameter using a combination of dry and wet sieving and retained grains with diameters falling within two narrow size ranges: "coarse" (125–210 μm) and "fine" (37–66 μm). The sorted mineral grains were rinsed with distilled-deionized (DDI) water and were dried in an oven at 50°C overnight.

Visual inspection of the crushed minerals under magnification showed that the quartz and hematite grains were generally angular in shape; however, the hematite tended to fracture into slightly more elongate grains than the quartz. Optical microscope images of the coarse grains are shown in Figure 3. We measured the specific surface area S_{SM} (surface area per unit mass of the solid phase) of the minerals with a Micromeritics ASAP 2020 Accelerated Surface Area and Porosimetry System using the Brunauer-Emmett-Teller (BET) adsorption method with nitrogen gas as the adsorbate. The values of S_{SM} and grain density δ, determined by helium pycnometry, for the crushed minerals are listed in Table 1. Samples having a heterogeneous mineralogy were created by mixing quartz and hematite grains of the same size to produce mixtures with nine hematite concentrations, represented as a volume fraction of the solid phase: 0, 0.005, 0.010, 0.020, 0.050, 0.100, 0.200, .0500, and 1. A specific solid-volume fraction θ_S of a mineral was achieved by

Downloaded 06 Oct 2011 to 171.67.216.22. Redistribution subject to SEG license or copyright; see Terms of Use at http://segdl.org/

controlling the mass m of the mineral constituents in each mixture and using experimentally determined values of grain density δ in the following mixture equation:

$$\theta_{S1} = \frac{m_1/\delta_1}{m_1/\delta_1 + m_2/\delta_2}, \quad (8)$$

where the subscript numbers denote either of the two mineral phases. For each of the nine concentrations, we created one coarse-grained mixture and one fine-grained mixture. Each mixture was gently tumbled for one minute to ensure that the mineral grains were evenly dispersed.

Dry samples of each mixture were packed into cylindrical Teflon sample holders with an inner diameter of 2.1 cm and a height of 6 cm. To achieve maximum saturation, packed samples were first evacuated for 30 minutes under a vacuum of 75 mm Hg. Samples were then submerged in a DDI water bath before atmospheric pressure was restored and were left to saturate for two hours. We determined the porosity ϕ of each sample gravimetrically, by comparing sample weights before and after saturation. We list ϕ values for the single-mineral quartz and hematite samples in Table 1 and values of S/V, where S is now the total surface area of the material and V is the total volume of the pore space. The ratio S/V is calculated using the following equation:

$$S/V = \frac{1-\phi}{\phi} S_{SM} \delta . \quad (9)$$

NMR measurements

We collected NMR T_2 relaxation measurements for all samples with a 2.2 MHz MARAN Ultra NMR core analyzer (manufactured by Resonance Instruments) using a CPMG pulse sequence. Each sample was placed in the analyzer for one hour before measurements were collected to equilibrate with the instrument temperature. Relaxation data were stacked 100 times to achieve a high signal-to-noise ratio ($\sim$150) and were consistently acquired at 30°C. The echo time (t_E) was varied ($t_E = 300$, 400, 600, and 800 μs) between repeated measurements to determine the magnitude of T_{2D}; however, only data for the shortest echo time $t_E = 300$ μs were used for subsequent detailed analysis. Directly after collecting measurements for each saturated sample, we extracted the pore fluid by centrifuging and collected independent relaxation measurements on the extracted fluid to determine T_{2B}.

The stacked CPMG decay signals were inverted to obtain T_2 distributions using a regularized, nonnegative least-squares Laplace transform algorithm developed after Whittall et al. (1991). In this algorithm, logarithmically sampled decay data are fit to 200 logarithmically spaced T_2 values, ranging from 0.1 ms to 10 s. The ill-posed inversion is regularized by minimizing the roughness of the resulting T_2 distribution. Regularization parameters were selected so that the residual data misfit appropriately matches the measured noise level.

EXPERIMENTAL RESULTS

Single-mineral samples

Before examining results for the heterogeneous mixtures, we first summarize results for the single-mineral samples, which serve as end members. For each single-mineral sample, we calculate the bulk fluid, surface, and diffusion relaxation rates (in equation 1) based on the mean log relaxation rate, using the approach of Keating and Knight (2007), and list these values in Table 1. Values of T_{2B}^{-1} are taken from measurements on the centrifuged pore fluid; T_{2D}^{-1} is determined using a linear regression of T_{2ml}^{-1} versus t_E^2 for measurements at varied echo time; T_{2S}^{-1} is determined from equation 1 after subtracting contributions from T_{2B}^{-1} and T_{2D}^{-1}. We also present values of ρ estimated from equation 3 using NMR-derived values of T_{2S}^{-1} and BET-derived values of S/V.

We find that estimated ρ values for hematite are nearly two orders of magnitude higher than those of quartz. This variation in ρ values agrees well with the data presented by Keating and Knight (2007). Thus, mixtures of these two minerals were confirmed to provide heterogeneous relaxation environments of interest in our study. We note that ρ values for the coarse- and fine-grained samples differ by about 20% for the quartz and 15% for the hematite. For the quartz samples, which contain few paramagnetic impurities, these differences likely reflect light surface contamination introduced during the crushing and sieving process. For the hematite samples, which are crushed from a natural mineral specimen, we expect that grains from different growth zones will differ in their exact mineralogy and thus exhibit a substantial range of ρ values.

An important consideration in the analysis of NMR data is determining whether the relaxation process can be described using the fast-diffusion approximation. Both quartz samples satisfy the condition for fast diffusion ($\rho r/D \ll 1$). Approximating an upper bound on the pore radius r as equivalent to the average grain radius, $\rho r/D = 0.087$ for the coarse quartz sample; for the fine quartz sample, $\rho r/D = 0.007$. The hematite samples, on the other hand, approach but do not strictly satisfy the fast-diffusion regime. For the coarse hematite sample, $\rho r/D = 1.73$; for the fine hematite sample, $\rho r/\mathrm{D} = 0.62$. Estimated values of ρ for the hematite should therefore be considered approximate, representing a reasonable lower bound on this parameter.

Table 1. Experimentally determined properties of the homogeneous end-member samples.

	Grain size	S_s (m^2/g)	δ (g/cm^3)	Φ	S/V (μm^{-1})	T_{2ml}^{-1} (s^{-1})	T_{2B}^{-1} (s^{-1})	T_{2D}^{-1} (s^{-1})	T_{2S}^{-1} (s^{-1})	ρ (μm/s)
Quartz	Coarse	0.161	2.61	0.442	0.530	0.619	0.328	0	0.291	0.549
	Fine	0.966	2.62	0.482	2.71	2.21	0.329	0	1.88	0.694
Hematite	Coarse	0.091	5.59	0.440	0.650	37.0	0.336	3.50	33.2	51.0
	Fine	0.610	5.61	0.479	3.71	227	0.348	5.60	221	59.7

Downloaded 06 Oct 2011 to 171.67.216.22. Redistribution subject to SEG license or copyright; see Terms of Use at http://segdl.org/

Full relaxation-time distributions for the four single-mineral samples are shown in Figure 4; the top row shows the quartz samples; the bottom row shows the hematite samples; the left and right columns correspond to the coarse- and fine-grained samples, respectively; and all distributions are normalized by the total signal amplitude. Both pure quartz samples exhibit a narrow distribution with a single peak positioned at long-T_2 values. The pure hematite samples, in contrast, exhibit broader distributions with multiple peaks spread over a range of short-T_2 values. Two factors likely contribute to the breadth of the hematite distributions. Foremost, as previously mentioned, we expect that the natural hematite grains do not all exhibit identical mineralogy and so might have widely varying values of ρ and surface area. Second, because the hematite samples do not strictly satisfy the condition of fast diffusion, surface relaxation will occur at more than one rate and so multiple or broadened peaks are expected to be observed.

One important result shown in Figure 4 is that, for a given grain size, the T_2 distributions for quartz and hematite do not overlap. Referring to the maximum relaxation time for the hematite distribution as $T_{H,MAX}$ and the minimum observed relaxation time for the quartz distribution as $T_{Q,MIN}$, we find that $T_{H,MAX} = 0.440$ s and $T_{Q,MIN} = 0.784$ s for the coarse-grained samples, and $T_{H,MAX} = 0.0488$ s and $T_{Q,MIN} = 0.207$ s for the fine-grained samples. The fact that the quartz and hematite distributions are thus distinct from one another allows us to devise a preliminary framework in which to analyze T_2 distributions for the quartz-hematite mixtures. Signals relaxing at T_2 values shorter than $T_{H,MAX}$ should correspond to spins that sample pore environments dominated by hematite surfaces. Signals exhibiting relaxation times longer than $T_{Q,MIN}$ should correspond to spins that sample only quartz surfaces. The presence of substantial signal relaxing at intermediate time ($T_{H,MAX} > T_2 > T_{Q,MIN}$) should indicate that these two relaxation environments are coupled by the diffusion of spins.

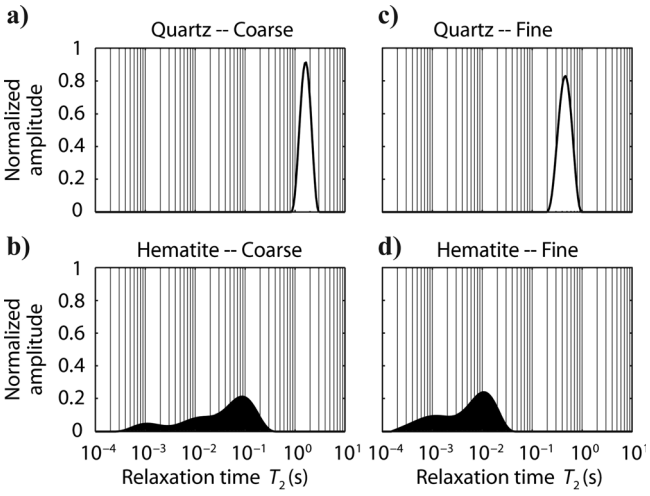

Figure 4. Experimentally determined T_2 distributions for the four homogeneous end-member samples: (a) coarse-grained quartz, (b) coarse-grained hematite, (c) fine-grained quartz, and (d) fine-grained hematite. All distributions are normalized by the total signal amplitude.

Heterogeneous samples

In Figure 5, we present T_2 distributions for the complete suite of heterogeneous samples in two columns: coarse-grained samples appear in the left column; fine-grained samples appear in the right column. Hematite concentrations increase downward with the volume fraction of the solid phase composed of hematite θ_{SH} listed at the center of each row. Distributions for the single-mineral samples are shown at the top (quartz) and bottom (hematite) of each column. All of the distributions are shaded to reflect the cutoff times defined above: signals relaxing at times shorter than $T_{H,MAX}$ are shaded black and are referred to as hematite signal; signals relaxing at times longer than $T_{Q,MIN}$ are shaded white and are referred to as quartz signal; gray shading is used for signals relaxing at intermediate times. We calculate the fraction of the total signal contained in each of these T_2 ranges and list these values in Table 2 as A_H, A_Q, and A_I, respectively. In addition to the shading, T_{2ml} for the pure quartz sample is displayed as a dashed vertical line over the columns of plots for each grain size.

Let us first consider the T_2 distributions for the coarse-grained heterogeneous samples (left column). We observe that distributions for the three samples with the lowest hematite concentration ($\theta_{SH} = 0.005$, 0.01, 0.02) exhibit similar characteristics. A tall narrow peak at long-T_2 values corresponds in position to the peak for pure quartz. A small amount of hematite signal is located at short T_2. The total amplitude of this hematite signal, indicated by A_H, increases in an approximately linear relationship with the hematite concentration. We note for these low concentrations of hematite, no signal exists at intermediate T_2 values and the bimodal mineralogy is generally discernible from the separate peaks in the distributions.

As the hematite concentration increases above $\theta_{SH} = 0.05$, the hematite signal continues to increase linearly in amplitude with θ_{SH}, and a distribution emerges which is similar to that of the pure hematite sample. The signal at long T_2, on the other hand, begins to broaden and shift toward shorter relaxation times that are no longer representative of the pure quartz sample. This change is reflected by an increase in the amplitude of intermediate signal A_I, relaxing at times between $T_{H,MAX}$ and $T_{Q,MIN}$. At a concentration of $\theta_{SH} = 0.20$, A_I exceeds 31%, and the distribution no longer conveys the presence of an underlying bimodal mineralogy. For the mixture with the highest concentration, $\theta_{SH} = 0.50$, there is no signal relaxing at times longer than $T_{Q,MIN}$, and the entire distribution closely resembles that of the pure hematite sample.

Distributions for the fine-grained samples (left column of Figure 5) exhibit patterns very similar to those observed for the coarse-grained samples. We note, however, that for samples with concentrations greater than $\theta_{SH} = 0.05$, a greater portion of the signal shifts from long relaxation times to intermediate relaxation times. At a concentration of $\theta_{SH} = 0.1$, for the fine-grained sample, the majority of the signal relaxes at intermediate times ($A_I = 58.1\%$); in comparison, $S_I = 19.0\%$ at this concentration for the coarse-grained sample. At a concentration of $\theta_{SH} = 0.2$, there is no signal relaxing at times longer than $T_{Q,MIN}$ for the fine-grained samples.

These experimental observations are generally compatible with the model illustrated in Figure 2, in which diffusional coupling is controlled by the relative magnitude of the separation

Downloaded 06 Oct 2011 to 171.67.216.22. Redistribution subject to SEG license or copyright; see Terms of Use at http://segdl.org/

length ℓ_S and the diffusion length ℓ_D, which varies with grain size and mineral concentration. At low hematite concentrations, we expect the separation length between hematite surfaces to be much greater than the diffusion length. Under this condition, most spins can sample only one mineralogy before relaxing, and thus we observe distinct peaks in the T_2 distribution that are reflective of the homogeneous quartz or hematite end members. As the hematite concentration increases, ℓ_S must eventually become shorter than ℓ_D. Under this condition, most spins become able to sample both quartz and hematite surfaces and so

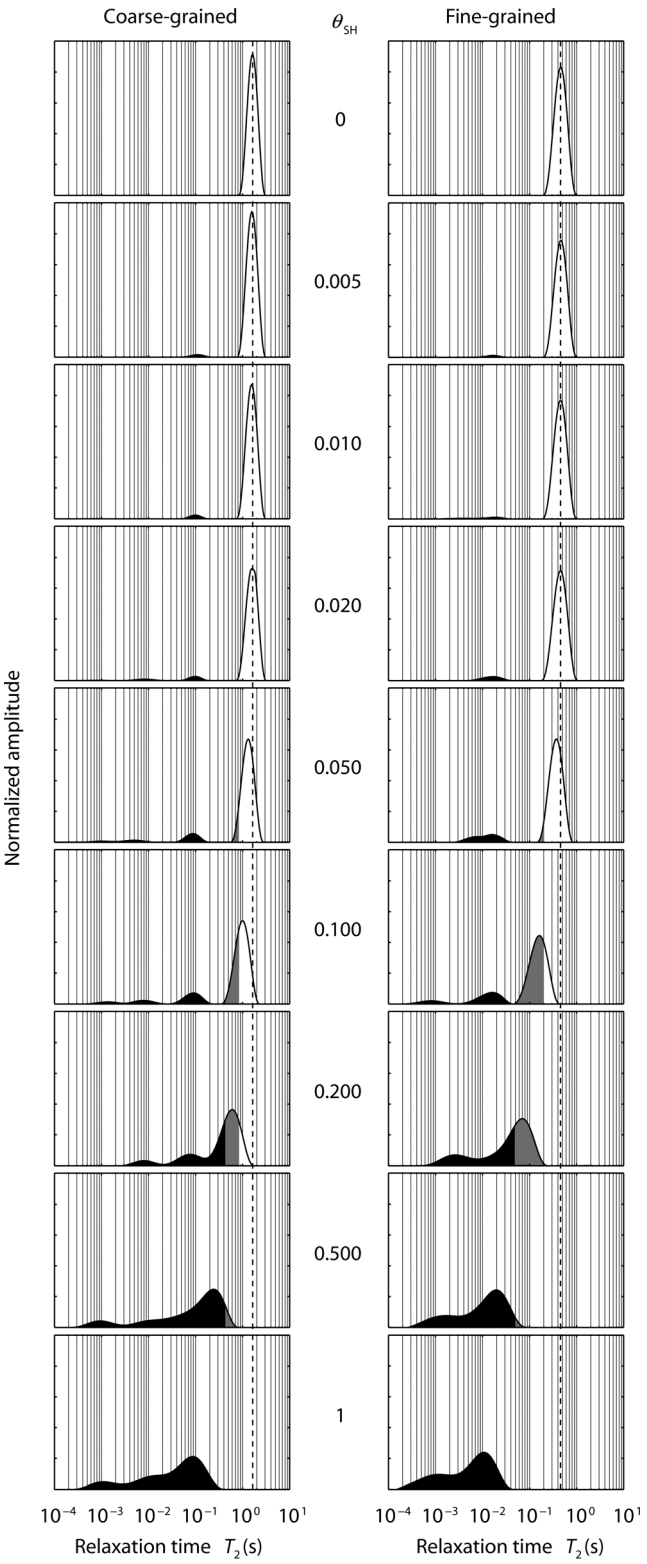

Figure 5. Experimentally determined T_2 distributions for the full suite of unconsolidated quartz-hematite mixtures and homogeneous end-member samples. Distributions in the left column correspond to the coarse-grained samples; those in the right column correspond to the fine-grained samples. The hematite concentration increases downward; θ_{SH} is listed at the center of each row. Shading reflects the cutoff times $T_{H,MAX}$ and $T_{Q,MIN}$: black shading reflects signals relaxing at times shorter than $T_{H,MAX}$; white shading reflects signals relaxing at times longer than $T_{Q,MIN}$; gray shading is used for signals relaxing at intermediate times. A dashed vertical line in each column of plots reflects the value T_{2Q}, calculated as the mean log relaxation time of the homogeneous quartz sample.

Table 2. Percentage of NMR signal classified as hematite signal (A_H), intermediate signal (A_I), and quartz signal (A_Q) for all experimental samples.

	θ_{SH}	$A_{H(\%)}$	$A_{I(\%)}$	$A_{Q(\%)}$
	0	0	0	100
	0.005	1.8	0	98.2
	0.010	2.7	0	97.4
	0.020	5.2	0	94.8
Coarse	0.050	11.3	2.5	86.2
	0.100	20.2	19.0	61
	0.200	49.5	31.1	20
	0.500	95.7	4.3	0
	1	100	0	0
	0	0	0	100
	0.005	1.4	0	98.6
	0.010	2.6	0	97.4
	0.020	4.7	0.1	95.2
Fine	0.050	12.2	2.2	85.6
	0.100	21	58.1	20.9
	0.200	53.5	46.2	0.2
	0.500	98.2	1.8	0
	1	100	0	0

Downloaded 06 Oct 2011 to 171.67.216.22. Redistribution subject to SEG license or copyright; see Terms of Use at http://segdl.org/

relax at intermediate times. Because the separation length also decreases with grain size, coupling is more significant for the fine-grained samples. These experimental results clearly demonstrate the importance and impact of diffusional coupling on NMR relaxation measurements in unconsolidated sediments.

ANALYSIS OF CRITICAL LENGTH SCALES IN HETEROGENEOUS SEDIMENTS

To quantify more directly how the relative magnitude of ℓ_S and ℓ_D influence the relaxation response for the samples, we consider how each length scale varies between the samples as a function of hematite concentration and grain size. This analysis provides insights into the link between the composition of an unconsolidated material and the length scales governing diffusional coupling, a necessary first step in accounting for this effect in the interpretation of NMR relaxation data.

We first consider the separation length ℓ_S. As a simple model, we approximate the hematite grains as uniform spheres evenly spaced at the centers of a cubic grid, as shown in Figure 6. This simplified model is generally appropriate for low hematite-concentration mixtures, when the spacing between hematite grains is not strongly dependent on packing geometry. The space between the hematite grains can be viewed as a continuum of quartz grains and pore space. In this arrangement, the side dimension of each model cube d can be calculated as

$$d = \left(\frac{4\pi}{3\theta_{SH}(1-\phi)}\right)^{1/3} r_g\,, \tag{10}$$

where r_g is the mean grain radius. The relevant separation length is the average distance a spin will diffuse before sampling a hematite surface. In a simple 1D system of separated plates, the mean distance a spin will diffuse to sample a plate surface is one-half the spacing between the plate surfaces. Thus, in this more complex 3D case, we approximate ℓ_S as the average distance from the face of the model cube, halfway between hematite grains, to the grain surface, given by

$$\frac{d}{2}\left(\int_0^1\int_0^1 \sqrt{x^2+y^2+1^2}\,dx\,dy\right) - r_g \approx \frac{d}{2}(1.28) - r_g\,. \tag{11}$$

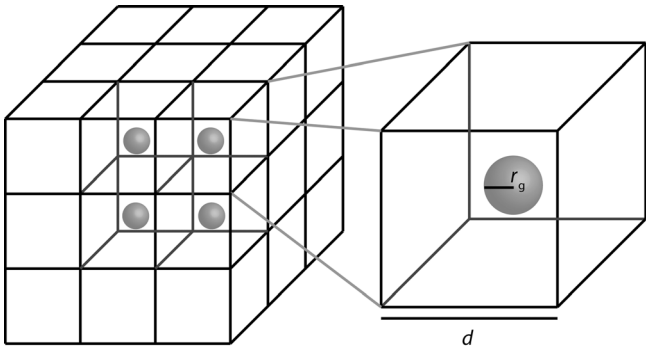

Figure 6. Illustration of the simplified model used to approximate ℓ_S. Gray hematite grains are approximated as spheres, having radius r_g, lying at the center of cubic unit cells, having uniform dimension d. The space between the hematite grains can be viewed as a continuum of quartz grains and pore space.

We note that this rough approximation of ℓ_S assumes uniform grain size and spacing, and does not take into account the tortuosity of the path between surfaces. In reality, the grains are not uniformly spaced, and some spread will occur in the distribution of ℓ_S values in each mixture.

Let us now consider the size of ℓ_D, the average distance a spin can diffuse (and potentially encounter a hematite surface) before relaxing. Because spins will eventually relax at quartz surface if they cannot reach a hematite surface, the maximum value for ℓ_D will be determined by the relaxation time of quartz. We thus calculate the upper limit for ℓ_D from equation 7 as

$$\ell_D \approx \sqrt{6DT_{2Q}}\,, \tag{12}$$

where T_{2Q} is the mean log relaxation time for the pure quartz sample and D is the self-diffusion coefficient of water at 30°C — 2.46×10^{-9} m^2/s (Simpson and Carr, 1958). We note that because T_{2Q} is shorter for the fine-grained quartz than for the coarse-grained quartz, ℓ_D is grain-size dependent and will be shorter in the fine-grained mixtures because spins will have a shorter time to diffuse before relaxing.

In Figure 7a, we plot values of ℓ_S and ℓ_D, estimated using the above equations for our laboratory samples; thick and fine lines correspond to the coarse- and fine-grained samples, respectively. The solid curves reflect the estimated value of ℓ_S as a function of θ_{SH}, and the dashed lines reflect the estimated value of ℓ_D. In Figure 7b, we show ℓ_S/ℓ_D as a function of θ_{SH}; $\ell_S/\ell_D<1$ indicates the existence of conditions that favor diffusional coupling. For the coarse-grained samples, when $\theta_{SH}>0.08$, $\ell_S/\ell_D<1$; for the fine-grained samples, when $\theta_{SH}>0.03$, $\ell_S/\ell_D<1$. We further note that for all concentrations, ℓ_S/ℓ_D is much less for the fine-grained samples than for the coarse-grained samples. For example, at an intermediate concentration of $\theta_{SH}=0.01$, ℓ_S/ℓ_D is $\sim$0.55 for the fine samples and $\sim$0.90 for the coarse samples.

Our experimental observations are consistent with this analysis of the variation in the critical length scales and the conceptual model shown in Figure 2. At concentrations where we predict $\ell_S/\ell_D<1$, we observe changes in the T_2 distributions consistent with the presence of diffusional coupling. The observation that coupling effects are more prevalent for the fine-grained mixtures is explained by the fact that ℓ_S/ℓ_D is significantly smaller for these samples. Analysis of the variation in ℓ_S/ℓ_D suggests that it might be possible to predict the extent of diffusional coupling given information about mineral concentration, surface relaxivity, and grain size. We note that whereas Figure 7 predicts coupling should be observed at lower concentrations for the finer grained mixtures, our experimental results show that coupling is first observed at a concentration of 5% for both grain sizes. This minor discrepancy could be attributed to the fact that the mean free path is shorter in the fine-grained samples; as such, ℓ_D will likely be overestimated by equation 12, which assumes unbound self-diffusion.

ANALYSIS OF RELAXATION TIMES IN HETEROGENEOUS SEDIMENTS

Having demonstrated how the extent of coupling varies with grain size and mineral concentration, we now more closely explore what specific information is conveyed by the T_2 distributions under these varied conditions. Although these systems are heterogeneous at the pore scale, we find that what is

Downloaded 06 Oct 2011 to 171.67.216.22. Redistribution subject to SEG license or copyright; see Terms of Use at http://segdl.org/

captured in the distributions depends on the relative magnitude of times that can be independently associated with relaxation at quartz surfaces and relaxation at hematite surfaces.

Let us first independently consider the time associated with relaxation at quartz surfaces. Because of the very low value of ρ, relaxation at quartz surfaces will always occur in the fast-diffusion regime, regardless of the concentration or spacing between quartz grains. This relaxation time associated with quartz surfaces is given by T_{2Q} and is equivalent to $\rho_Q S_Q/V$, where ρ_Q and S_Q are, respectively, the relaxivity and the surface area of quartz. Let us next independently consider the time associated with relaxation at hematite surfaces. Relaxation at hematite surfaces, which have a high value of ρ, requires a short separation distance between hematite surfaces to satisfy the condition for fast diffusion. At high hematite concentrations, when hematite surfaces are closely spaced, this condition is nearly met and the relaxation time T_{2H} will be approximated by $\rho_H S_H/V$, where ρ_H and S_H are, respectively, the relaxivity and the surface area of hematite. At low hematite concentrations, on the other hand, hematite grains are sparsely distributed, and the distance separating hematite surfaces is sufficiently long that relaxation with respect to these surfaces will be limited by diffusion.

In the diffusion-limited regime, the decay time of the dominant mode associated with the high-ρ surface will be proportional to the mean-squared distance a spin will diffuse to a reach the relaxing surface. We refer to this relaxation time, in our analysis of the hematite-quartz systems, as $T_{2H,slow}$ and estimate the magnitude of this time as follows:

$$T_{2H,slow}^{-1} \approx \frac{6D}{\ell_S^2}, \tag{13}$$

where we have taken equation 4, describing slow diffusion in a single pore, and replaced the pore radius r with the separation length ℓ_S. In addition to this dominant relaxation mode, there also exist higher order modes that will exhibit shorter relaxation times related to ρ of the hematite surface.

When we consider a mixture of hematite and quartz, the relative magnitudes of these relaxation times determine the overall response of the heterogeneous system. Specifically, the relaxation process that is characterized by the shortest time will dominate the overall relaxation response. For mixtures with a low concentration of hematite, ℓ_S is large, so (as seen in equation 13) $T_{2H,slow} \gg T_{2Q}$. As a result, relaxation at quartz surfaces limits the maximum observed relaxation time to T_{2Q}. The peak at long T_2 thus directly reflects T_{2Q} and the relaxation response of the homogeneous quartz sample. The relaxation mode given by $T_{2H,slow}$ does not contribute significantly to relaxation; however, a portion of the signal relaxing at short T_2 corresponds to the higher order modes of relaxation at hematite surfaces in the slow-diffusion regime. These modes exhibit shorter relaxation times, and are roughly representative of the T_2 distribution for the pure hematite sample. The amplitude of the signal in these modes, given by S_H, increases linearly with θ_{SH} and approximately reflects the volume fraction of water, which can diffuse to a nearby hematite surface within the relaxation time associated with these higher order modes. For the low-θ_{SH} samples, the observed T_2 distribution thus captures, independently, the relaxation properties of the two mineral constituents and thus directly reflects the heterogeneous nature of the mixtures.

As the hematite concentration increases and ℓ_S decreases, $T_{2H,slow}$ eventually becomes shorter than T_{2Q}. We note that the condition $T_{2H,slow} < T_{2Q}$, as defined here, is equivalent to the condition $\ell_S/\ell_D < 1$, in which diffusional coupling effects become apparent (i.e., both conditions indicate $\ell_S^2/6D < T_{Q.}$). At this critical point, the maximum observed relaxation time becomes limited by $T_{2H,slow}$ instead of T_{2Q}. Therefore, the long-T_2 peak shifts to a time that is a function of ℓ_S, describing the distance between hematite surfaces, instead of $\rho S/V$ for either mineral constituent. The signal at short T_2 still reflects the higher order modes representative of the pure hematite samples.

As the hematite concentration continues to increase, hematite grains are more closely spaced, and ℓ_S decreases to a point that relaxation at hematite surfaces approaches the fast-diffusion regime. McCall et al. (1991) theorize that in the condition of fast diffusion and strong coupling, the relaxation rate of a heterogeneous system will reflect the average value of $\rho S/V$ for the entire pore space; i.e., we can write the following approximate model equation:

$$T_2^{-1} \approx \rho \frac{S}{V} \approx (\rho_H S_H + \rho_Q S_Q)/V. \tag{14}$$

Because $\rho_H \gg \rho_Q$, the term $\rho_Q S_Q$ can be neglected and, in the case of strong coupling and fast diffusion, the average value of T_2^{-1} is expected to become a linear function of the surface area composed of hematite, which is approximated by θ_{SH}.

In Figure 8, we plot the mean log relaxation rate T_{2ml}^{-1} versus θ_{SH} for the (a) coarse and (b) fine samples. The dashed gray line

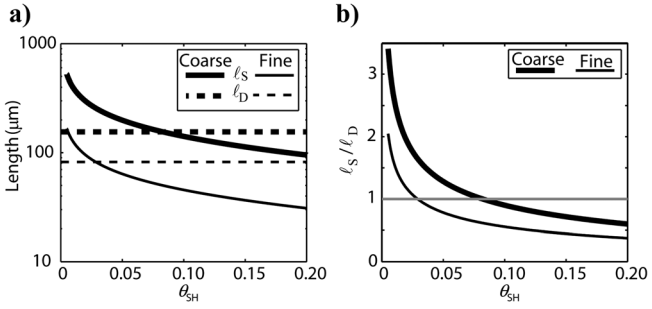

Figure 7. Comparison of theoretically approximated values of the ℓ_S and ℓ_D for the laboratory samples. Coarse and fine lines correspond to the coarse- and fine-grained samples, respectively. (a) Solid lines show the estimated value of ℓ_S as a function of θ_{SH}; dashed lines reflect the estimated value of ℓ_D. (b) Solid lines show the estimated ratio ℓ_S/ℓ_D; a gray line at $\ell_S/\ell_D = 1$ is provided for reference.

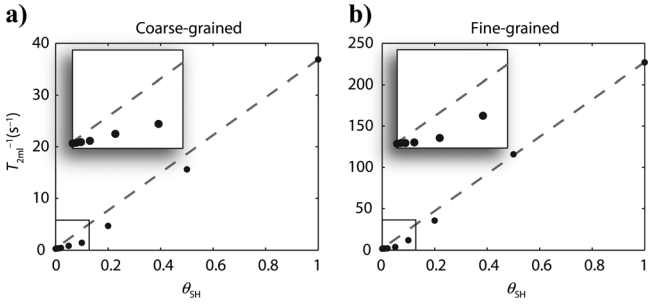

Figure 8. The mean log relaxation time plotted versus θ_{SH} for the (a) coarse-grained and (b) fine-grained samples. The dashed gray line connects points at $\theta_{SH} = 0$ and $\theta_{SH} = 1$ and approximates the trend of the average value of $\rho S/V$. Inset plots show higher detail for points with low hematite concentrations of $\theta_{SH} = 0$ to $\theta_{SH} = 0.100$.

Downloaded 06 Oct 2011 to 171.67.216.22. Redistribution subject to SEG license or copyright; see Terms of Use at http://segdl.org/

connecting the points at $\theta_{SH}=0$ and $\theta_{SH}=1$ displays the trend in $\rho_H S_H$, which approximates the average value of $\rho S/V$ for the pore space. We find that for the high-concentration mixtures in which coupling is strong (θ_{SH} greater than $\sim$0.1), the observed values of T_{2ml}^{-1} generally follow this trend, and thus convey the relative mineral concentrations and the average value of $\rho S/V$. For the low-concentration samples, which are not in the fast-diffusion, strong-coupling limit, T_{2ml}^{-1} follows a shallower slope, and T_{2ml}^{-1} is skewed toward $\rho_Q S_Q$ instead of the average $\rho S/V$ of the mixtures. In comparison to our results, analytic and numerical results from Ryu and Johnson (2009) suggest that an average value of T_2^{-1} will not always provide a reliable indication of pore-scale heterogeneity in ρ, and that the heterogeneous character of the pore space tends to be more directly apparent in the slope of the relaxation decay at late times only.

Our findings demonstrate that the relaxation-time distribution in heterogeneous sediments provides fundamentally different information depending on the relative magnitude of critical length scales and the extent of diffusional coupling. For conditions in which coupling is weak, the relaxation-time distribution captures the heterogeneous nature of the sediments and independently conveys the relaxation properties of the sample constituents. When coupling is strong, the underlying heterogeneity is obscured, and the measured relaxation times instead reflect the averaged relaxation properties of the medium. These averaged relaxation properties are most strongly influenced by the distribution of the fastest relaxing surfaces; in the systems considered here, fast-relaxing hematite surfaces dominate the relaxation response. We have shown that in unconsolidated sediments with a heterogeneous mineralogy, the extent of coupling will depend largely on the relative concentrations of the mineral phases, their ρ-value, and grain size. This information thus can be used to estimate the magnitude of coupling, and to account for this process in the interpretation of the measured NMR relaxation times.

Here, we have explored systems in which the measured relaxation rates and the influence of heterogeneity are dominated by the surface relaxation process. We note that the presence of minerals with considerable magnetic susceptibility can give rise to an additional relaxation process associated with an inhomogeneous internal magnetic field. These magnetic relaxation effects will further influence the measured relaxation time T_2 (Keating and Knight, 2008) and have a particularly pronounced effect on the relaxation time T_2^* (Grunewald and Knight, 2011), which is measured most directly by surface-based NMR instruments. Further work is required to understand how the magnetic susceptibility of the grains will influence measured relaxation times in heterogeneous systems.

CONCLUSIONS

Measurements of NMR relaxation times provide a unique perspective into the pore space of geologic media. Following decades of NMR applications in petroleum well logging, there exists a growing interest in using borehole and surface-based NMR techniques to characterize pore-scale properties of geologic materials in the critical zone of the earth's near surface. Successful interpretation of these measurements, however, requires a more complete understanding of the factors controlling the NMR relaxation response in the geologic materials most commonly encountered in these environments. In this study, we have focused on investigating NMR relaxation times in unconsolidated heterogeneous sediments, and more specifically, sediments with a bimodal mineralogy.

Our laboratory experiments, using controlled mixtures of quartz and hematite grains, demonstrate that the information conveyed by the relaxation-time distribution in these materials depends critically on the magnitude of two key length scales affecting the process of diffusional coupling: the diffusion length and the separation length. When the separation length is much longer than the diffusion length, the relaxation-time distribution conveys the heterogeneous character of the mixtures and independently reflects the relaxation properties of the two mixture constituents. When the separation length is much shorter than the diffusion length, diffusional coupling obscures the heterogeneous character of the mixture; however, the average relaxation properties are captured more directly by the measured relaxation time. The extent of coupling is shown to be highly dependent on the mineral concentration and grain size, both of which strongly influence the magnitude of the separation length. This study complements one of our previous laboratory studies, which explores how variation in the diffusion length influences the extent of coupling.

The manner in which heterogeneity is reflected by the relaxation-time distribution has important implications for the estimation of pore-scale parameters from measured relaxation times. In certain situations, pore-scale parameters might most accurately be derived based on the average relaxation properties of the pore space, conveyed in the case of strong coupling. In other cases, these parameters might depend most strongly on the properties of the individual heterogeneous components, conveyed only under conditions of weak coupling. As an example, permeability, which is estimated using the link between the surface relaxation rate and the surface-area-to-volume ratio S/V, will in some cases be dependent on the average value of S/V, and in other cases might be more strongly influenced by S/V in a particular region of the pore space (e.g., the largest or smallest pores). We note that because mineralogy and pore geometry both control the surface relaxation rate ($\rho S/V$), our samples with uniform pore geometry and heterogeneous mineralogy (ρ) are roughly analogous in their NMR behavior to samples with uniform ρ and heterogeneous pore geometry (S/V). In practice, the relaxation-time distributions can reflect heterogeneity in ρ, heterogeneity in S/V, or heterogeneity in both of these parameters.

These experiments have considered relatively simple, well-characterized materials that allow us to explore systematically the factors controlling the NMR response over a wide but controlled range of conditions. Specifically, we have investigated unconsolidated sediments in which heterogeneity occurs with varying mineralogy between grains; however, we note that heterogeneity could occur in other forms in nature (e.g., heterogeneous surface mineralogy on the surface of a single grain). We expect that the fundamental factors identified in this study will also be critical to determining the relaxation response in other geologic materials, including consolidated rocks as well as other unconsolidated sediments. In future research, it will be especially valuable to extend the framework of this study to explore directly the NMR relaxation response of natural unconsolidated sediments containing magnetic minerals. Continued research in this area will serve to advance the use of NMR as a powerful investigative tool in near-surface applications.

Downloaded 06 Oct 2011 to 171.67.216.22. Redistribution subject to SEG license or copyright; see Terms of Use at http://segdl.org/

ACKNOWLEDGMENTS

This material is based on work supported by the National Science Foundation under Grant No. EAR-0911234. Any opinions, findings, and conclusions or recommendations expressed in this material are those of the authors and do not necessarily reflect the views of the National Science Foundation. Further funding was provided by Schlumberger Water Services and by a graduate research grant to E. Grunewald from BP, PLC. We thank the Stanford Surface and Aqueous Geochemistry Group for use of their surface area. We appreciate helpful comments contributed by three anonymous reviewers.

REFERENCES

Anand, V., and G. J. Hirasaki, 2007, Diffusional coupling between micro and macroporosity for NMR relaxation in sandstones and grainstones: Petrophysics, **48**, no. 4, 289–307.

Bloembergen, N., E. M. Purcell, and R. V. Pound, 1948, Relaxation effects in nuclear magnetic resonance absorption: Physical Review, **73**, no. 7, 679–712, doi:10.1103/PhysRev.73.679.

Borgia, G. C., V. Bortolotti, A. F. Brancolini, R. J. S. Brown, and P. Fantazzini, 1996, Developments in core analysis by NMR measurements: Magnetic Resonance Imaging, **14**, no. 7-8, 751–760, doi:10.1016/S0730-725X(96)00160-9.

Brownstein, K. R., and C. E. Tarr, 1979, Importance of classical diffusion in NMR studies of water in biological cells: Physical Review A, **19**, no. 6, 2446–2453, doi:10.1103/PhysRevA.19.2446.

Bryar, T. R., C. J. Daughney, and R. J. Knight, 2000, Paramagnetic effects of iron (III) species on nuclear magnetic relaxation of fluid protons in porous media: Journal of Magnetic Resonance, **142**, no. 1, 74–85, doi:10.1006/jmre.1999.1917.

Carr, H. Y., and E. M. Purcell, 1954, Effects of diffusion on free precession in nuclear magnetic resonance experiments: Physical Review, **94**, no. 3, 630–638, doi:10.1103/PhysRev.94.630.

Cohen, M. H., and K. S. Mendelson, 1982, Nuclear magnetic relaxation and the internal geometry of sedimentary rocks: Journal of Applied Physics, **53**, no. 2, 1127–1135, doi:10.1063/1.330526.

Davies, S., M. Z. Kalam, K. J. Packer, and F. O. Zelaya, 1990, Pore-size distributions from nuclear magnetic resonance spin-lattice relaxation measurements of fluid-saturated porous solids: 2 — Application to reservoir core samples: Journal of Applied Physics, **67**, 3171–3176.

D'Orazio, F., J. C. Tarczon, W. P. Halperin, K. Eguchi, and T. Mizusaki, 1989, Application of nuclear magnetic resonance pore structure analysis to porous silica glass: Journal of Applied Physics, **65**, no. 2, 742–751, doi:10.1063/1.343088.

Fleury, M., and J. Soualem, 2009, Quantitative analysis of diffusional pore coupling from T2-store-T2 NMR experiments: Journal of Colloid and Interface Science, **336**, no. 1, 250–259, doi:10.1016/j.jcis.2009.03.051.

Foley, I., S. A. Farooqui, and R. L. Kleinberg, 1996, Effect of paramagnetic ions on NMR relaxation of fluids at solid surfaces: Journal of Magnetic Resonance, Series A, **123**, no. 1, 95–104, doi:10.1006/jmra.1996.0218.

Gallegos, D. P., and D. M. Smith, 1988, A NMR technique for the analysis of pore structure: Determination of continuous pore size distributions: Journal of Colloid and Interface Science, **122**, no. 1, 143–153, doi:10.1016/0021-9797(88)90297-4.

Godefroy, S., J. P. Korb, M. Fleury, and R. G. Bryant, 2001, Surface nuclear magnetic relaxation and dynamics of water and oil in macroporous media: Physical Review E: Statistical, Nonlinear, and Soft Matter Physics, **64**, no. 2, 021605, doi:10.1103/PhysRevE.64.021605.

Grunewald, E., and R. Knight, 2009, A laboratory study of NMR relaxation times and pore coupling in heterogeneous media: Geophysics, **74**, no. 6, E215–E221, doi:10.1190/1.3223712.

——, 2011, The effect of pore size and magnetic susceptibility on the surface NMR relaxation parameter T_2*: Near Surface Geophysics, **9**, doi:10.3997/1873-0604.2010062.

Hertrich, M., 2008, Imaging of groundwater with nuclear magnetic resonance: Progress in Nuclear Magnetic Resonance Spectroscopy, **53**, no. 4, 227–248, doi:10.1016/j.pnmrs.2008.01.002.

Keating, K., and R. Knight, 2007, A laboratory study to determine the effect of iron oxides on proton NMR measurements: Geophysics, **72**, no. 1, E27–E32, doi:10.1190/1.2399445.

——, 2008, A laboratory study of the effect of magnetite on NMR relaxation rates: Journal of Applied Geophysics, **66**, no. 3-4, 188–196.

Keating, K., R. Knight, and K. Tufano, 2008, Nuclear magnetic resonance relaxation measurements as a means of monitoring iron mineralization processes: Geophysical Research Letters, **35**, no. 19, L19405, doi:10.1029/2008GL035225.

Kenyon, W. E., P. I. Day, C. Straley, and J. F. Willemsen, 1988, A three-part study of NMR longitudinal relaxation properties of water-saturated sandstones: SPE Formation Evaluation, **3**, no. 3, 622–636, doi:10.2118/15643-PA.

Kleinberg, R. L., and M. A. Horsfield, 1990, Transverse relaxation processes in porous sedimentary rock: Journal of Magnetic Resonance, **88**, 9–19.

Legchenko, A., and P. Valla, 2002, A review of the basic principles for proton magnetic resonance sounding measurements: Journal of Applied Geophysics, **50**, no. 1-2, 3–19, doi:10.1016/S0926-9851(02)00127-1.

Maliva, R., E. Clayton, and T. Missimer, 2009, Application of advanced borehole geophysical logging to managed aquifer recharge investigations: Hydrogeology Journal, **17**, no. 6, 1547–1556, doi:10.1007/s10040-009-0437-z.

McCall, K. R., D. L. Johnson, and R. A. Guyer, 1991, Magnetization evolution in connected pore systems: Physical Review B: Condensed Matter and Materials Physics, **44**, no. 14, 7344–7355, doi:10.1103/PhysRevB.44.7344.

Meiboom, S., and D. Gill, 1958, Modified spin-echo method for measuring nuclear relaxation times: Review of Scientific Instruments, **29**, no. 8, 688–691, doi:10.1063/1.1716296.

Ryu, S., and D. L. Johnson, 2009, Aspects of diffusion-relaxation dynamics with a nonuniform, partially absorbing boundary in general porous media: Physical Review Letters, **103**, no. 11, 118701, doi:10.1103/PhysRevLett.103.118701.

Seevers, D. O., 1966, A nuclear magnetic method for determining the permeability of sandstones: 33rd Annual Logging Symposium, Society of Professional Well Log Analysts, Transactions, Paper L.

Senturia, S. D., and J. D. Robinson, 1970, Nuclear spin-lattice relaxation of liquids confined in porous solids: SPE Journal, **10**, 237–244.

Simpson, J. H., and H. Y. Carr, 1958, Diffusion and nuclear spin relaxation in water: Physical Review, **111**, no. 5, 1201–1202, doi:10.1103/PhysRev.111.1201.

Stucki, J. W., B. A. Goodman, and U. Schwertmann, 1988, Iron in soil and clay minerals: D. Reidel Publishing Co.

Timur, A., 1969, Pulsed nuclear magnetic resonance studies of porosity, movable fluid, and permeability of sandstone: Journal of Petroleum Technology, **21**, no. 6, 755–786, doi:10.2118/2045-PA.

Toumelin, E.,C. Torres-Verdin, S. Chen, and D. M. Fischer, 2002, Analysis of NMR diffusion coupling effects in two-phase carbonate rocks: Comparison of measurements with Monte Carlo simulations: 43rd Annual Logging Symposium, Society of Professional Well Log Analysts, Transactions, Paper JJJ.

Walsh, D. O., 2008, Multi-channel surface NMR instrumentation and software for 1D/2D groundwater investigations: Journal of Applied Geophysics, **66**, no. 3-4, 140–150, doi:10.1016/j.jappgeo.2008.03.006.

Walsh, D. O., E. Grunewald, P. Turner, and I. Frid, 2010, Javelin: A slim-hole and microhole NMR logging tool: FastTimes, **15**, no. 3, 67–72.

Whittall, K. P., M. J. Bronskill, and R. M. Henkelman, 1991, Investigations of analysis techniques for complicated NMR relaxation data: Journal of Magnetic Resonance (San Diego, Calif.), **95**, 221–234.

Zielinksi, L. J., Y.-Q. Song, S. Ryu, and P. N. Sen, 2002, Characterization of coupled pore systems from the diffusion eigenspectrum: Journal of Chemical Physics, **117**, no. 11, 5361–5365, doi:10.1063/1.1499956.

Downloaded 06 Oct 2011 to 171.67.216.22. Redistribution subject to SEG license or copyright; see Terms of Use at http://segdl.org/